ISSN 2070-2051, Protection of Metals and Physical Chemistry of Surfaces, 2021, Vol. 57, No. 1, pp. 88–95. © Pleiades Publishing, Ltd., 2021.
Russian Text © The Author(s), 2021, published in Fizikokhimiya Poverkhnosti i Zashchita Materialov, 2021, Vol. 57, No. 1, pp. 86–93.

NEW SUBSTANCES, MATERIALS, AND COATINGS

Physicochemical and Biocidal Properties of Nickel–Tin and Nickel–Tin–Titania Coatings

A. V. Pyanko[a, *], I. V. Makarova[b], D. S. Kharitonov[c], I. S. Makeeva[d], D. S. Sergievich[a], and A. A. Chernik[a]

[a] *Belarusian State Technological University, Minsk, 220006 Belarus*
[b] *Lappeenranta University of Technology, Lappeenranta, 53-850 Finland*
[c] *Jerzy Haber Institute of Catalysis and Surface Chemistry, Polish Academy of Sciences, Krakow, 30-239 Poland*
[d] *Kyiv National University of Technologies and Design, Kyiv, 01011 Ukraine*
**e-mail: hanna.pianka@mail.ru*

Received May 12, 2020; revised June 1, 2020; accepted June 8, 2020

Abstract—The morphology and composition of Ni–Sn and Ni–Sn–TiO_2 coatings have been studied by scanning electron microscopy and energy-dispersive X-ray analysis. The electrochemical behavior of the obtained coatings in a 3% NaCl solution has been examined. The influence of the inclusion of titania in the Ni–Sn coating on the mechanical and antibacterial properties has been revealed. Dependences of the influence of incubation time and exposure to UV radiation on the concentration of living bacteria cells on the surface of the Ni–Sn–TiO_2 coating have been established. In bacterial tests with Ni–Sn–TiO_2 coatings deposited from the electrolyte containing 2 g/L TiO_2, the concentration of viable *Staphylococcus aureus* decreases from 130 to 90 CFU/mL and from 70 to 30 CFU/mL without and with UV irradiation, respectively.

Keywords: alloy, nickel–tin, titania, corrosion, biocidal properties

DOI: 10.1134/S2070205121010160

INTRODUCTION

According to the World Health Organization [1, 2], more than 1 billion people annually have infectious diseases, of which from 290000 to 650000 people die due to complications. The spread of infectious diseases depends on many factors [3–5]. The most significant are the epidemiological situation in a country, the degree of contagiousness of the disease, and climatic conditions. The degree of contagiousness, in turn, depends on the transmission path of the disease, one of which is the contact path [6, 7]. In this case, the pathogen is transmitted through the skin by direct contact or contacted surfaces (handrails, door handles, etc.) [1–14]. Thus, the development of a new class of metal composite materials with antibacterial properties is a promising direction in the field of materials science.

Composite materials based on Cu [15–18], Ni [19–23], and Fe [19, 20] metallic substrates can be used as antibacterial coatings. Relevantly, nickel–tin alloys have high corrosion resistance and do not irritate human skin [10–14]. In our previous work [24], the mechanism of nickel–tin alloy formation and its structure and morphology were described. This alloy is used in industry as a protective and decorative coating for copper and steel products [25, 26].

As an inert phase for composite coatings, TiO_2 [27–29], SiC [30, 31], and Ag [32, 33] nanoparticles are commonly used. Composite coatings with such nanoparticles show high efficiency against resistant bacteria [13, 34–36] due to the suppression of the vital activity of the causative agent of the infectious disease as a result of inhibition of the metabolic process specific to particular microorganisms [7].

Due to its unique properties, nanosized TiO_2 is widely used as a photocatalyst for the decomposition of organic pollutants and inhibitors of microorganisms [37, 38]. The widespread use of TiO_2 is based on its effective photocatalytic activity [39–41] and high chemical stability [42–44]. In works [42–48], its antibacterial efficacy under the influence of UV radiation has been studied. It should be noted that titanium oxide, which naturally occurs in various modifications (anatase, rutile, brookite), as a rule, is not a photocatalyst. To impart photocatalytic properties, TiO_2 must be synthesized under certain conditions and have a nanoscale structure. In [39–41], it has been shown that TiO_2 particles with sizes ranging from 10 to 50 nm have the highest photocatalytic activity.

Thus, electrochemically formed nickel–tin alloys have several advantages over individual metal coatings. The introduction of nanosized titania into the alloy

structure will impart the metal surface a number of unique properties. In this regard, the purpose of this work was to study the mechanical, tribological, corrosion, and antibacterial properties of nickel–tin and nickel–tin–titania coatings.

EXPERIMENTAL

Nickel–tin and nickel–tin–titania coatings were electrochemically deposited from electrolytes following the procedure reported elsewhere [24]. Tin and nickel plates with an area ratio of 1 : 5 were used as anodes. The coatings were deposited on copper and steel plates prepared in accordance with GOST (State Standard) 9.305–84.

Nanosized titania was synthesized by direct oxidation of powdered metallic titanium according to the procedure [49]. As a result, a mixture of two polymorphic modifications of titania, namely anatase and rutile, with a particle size of 30–50 nm was obtained [50].

Electrochemical measurements were performed using an Autolab PGSTAT 302N potentiostat in a three-electrode cell with a saturated silver-silver chloride reference electrode and a platinum counter electrode. A 3% NaCl solution was used as a corrosive medium. Polarization curves were recorded at a potential sweep rate of 1 mV/s after the open-circuit potential (OCP) was established for 30 min. Electrochemical impedance spectra were recorded in a frequency range from 10 kHz to 0.01 Hz with an ac voltage amplitude of 10 mV. The frequency impedance spectra were recorded after 30 min of the corrosion test. The obtained data were processed using the Nova 2.1 software.

The surface morphology of the obtained samples was examined by scanning electron microscopy (SEM) on a JEOL JSM–5610 LV microscope and by atomic force microscopy (AFM) on a Nanosurf FlexAxiom setup with a C3000 controller in the semicontact mode using a silicon *n*-type cantilever with a needle tip radius of 8 nm (HQ: NSC15, MikroMasch). The elemental composition of the coatings was determined by energy-dispersive X-ray microanalysis (EDX) using an EDX JED-2201 chemical microprobe analysis system.

The adhesion of Ni–Sn and Ni–Sn–TiO_2 coatings to the steel substrate was measured with a Defelsko Positest AT adhesion meter and tested by the method of a grid of scratches and bending.

The microhardness of 20-μm-thick coatings was measured with an AFFRI-MVDM8 microhardness tester according to *GOST* (State Standard) 2999-75 with a load on the indenter of 50 g.

The antibacterial properties of the coatings were studied against gram-positive *Staphylococcus aureus* (*S. aureus*, ATCC 6538) and gram-negative *Escherichia coli* (*E. coli*, ATCC 8739) bacteria. Before antibacterial studies, the surface of the samples was sterilized in ethanol (70%) for 2 h and dried at room temperature under UV irradiation.

Tested bacteria (one colony) were transferred into a test tube with 2 mL of culture medium and the number of bacteria was determined. The liquid with bacteria was diluted so that the resulting solution contained from 5.5×10^5 to 2.5×10^6 CFU/mL of bacteria. This solution was used as a test liquid. Then, 0.1 mL of the test liquid was inoculated onto the test sample, covered with a film, and lightly pressed so that the liquid was distributed over the entire surface. The sample was irradiated for 1 h at ultraviolet radiation with the intensity of ~0.01 mW/cm^2 and a temperature of 20 ± 1°C. Afterward, samples were rinsed in sterile plastic bags containing 10 mL of physiological solution and Triton X-100 (0.1% concentration) for 10 min. The washed-off liquid (0.1 mL) was immediately plated on nutrient agar in a Petri dish with a sterile pipette. The solution was distributed over the agar medium and the cups were covered with a lid and left at room temperature for 5 min. Then, the seeded dishes were placed in a thermostat and incubated for 48 h at a temperature of 30 ± 1°C. The number of formed bacteria colonies was counted, and the concentration of bacteria in the washing liquid was established.

The antibacterial activity of coatings was assessed using parameters K_1 and K_2:

$$K_1 = 100 \times (C_{cont} - C_{ex})/C_{cont}, \quad (1)$$

$$K_2 = \log(C_{cont}/C_{ex}), \quad (2)$$

where C_{cont} and C_{ex} are, respectively, concentrations of bacteria after incubation on a reference sample and examined composite (CFU/mL).

The antibacterial activity of the coated plates was also evaluated without exposure to UV radiation. For this, sterile plates were placed in bags with 20 mL of test bacteria (*S. aureus* and *E. coli*) previously diluted to a concentration of 10^5 CFU/mL and incubated for 4 and 12 h at 30°C. Seeding was then carried out from the corresponding dilutions. Inoculations were incubated for 24 h at a temperature of 30°C.

RESULTS AND DISCUSSION

Nickel–tin (Fig. 1a) and nickel–tin–titanium-dioxide alloys (Fig. 1b) were deposited as smooth, shiny, and well-adhered coatings with a dense uniform structure. The introduction of TiO_2 into the electrolyte lead to an insignificant change in the appearance of the coating; the formation of rather large spheroids of 6–8 μm in size was observed on the surface. According to elemental analysis data, the obtained Ni–Sn coatings contain 68–73 wt % of tin and 26–31 wt % of nickel. These ratios are optimal, since in this case a mechanical mixture of $NiSn_2$ and Ni_3Sn_2 is formed [24, 51].

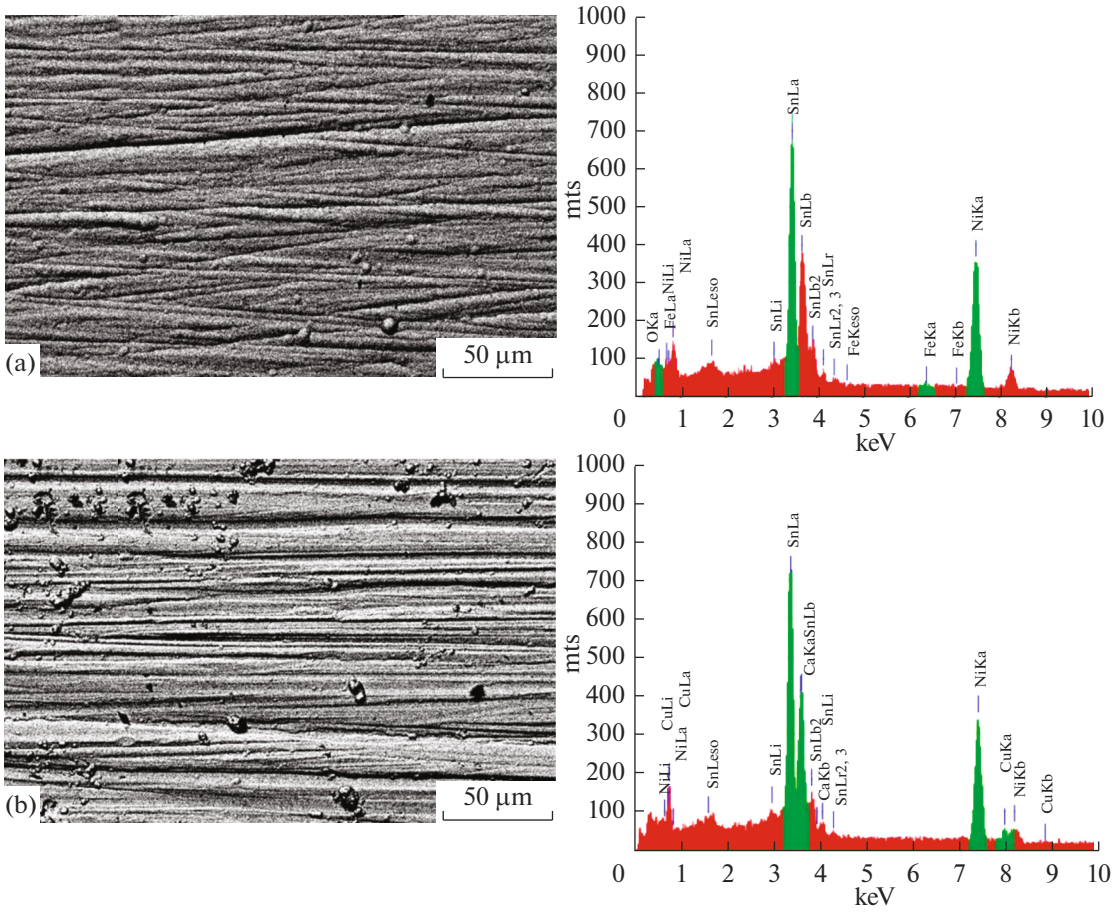

Fig. 1. Microstructure and elemental analysis of (a) Ni–Sn and (b) Ni–Sn–TiO_2 coatings.

The introduction of TiO_2 into the electrolyte leads to a change in the structure of the coating surface with an enlargement of crystallites formed on the surface. As follows from the AFM data (Fig. 2), an increase in the TiO_2 content in the electrolyte from 0 to 2 g/L leads to the growth of individual crystallites from 25 to 30 nm.

The adhesion and microhardness of the Ni–Sn and Ni–Sn–TiO_2 coatings are presented in Table 1. The microhardness of the Ni–Sn coating was 405 HV, and the adhesion was 0.51 MPa/cm^2. Introduction of TiO_2 in the electrolyte leads to an increase in the microhardness and adhesion to 439 HV and 0.65 MPa/cm^2, respectively.

Polarization curves of the alloys obtained in the 3% NaCl solution are shown in Fig. 3. The cathode branches of the polarization curves practically coincide, which indicates an insignificant effect of the composition and structure of the coating on the cathodic process.

However, a significant shift to the electropositive side was observed on anodic polarization curves when TiO_2 was introduced into the electrolyte. Thus, the beginning of the anodic process for samples without and with TiO_2 is observed in the range of –50 and –25 mV, respectively, while the alloy with TiO_2 had a more positive OCP. At the anodic polarization of +50 mV, a region of relative passivation was observed for the nickel–tin alloy in the potential range of 50–300 mV with a slope of approximately 0.4 V. The introduction of TiO_2 into the electrolyte leads to the surface activation in the potential range of 0–0.2 V. The slope of the polarization curves in this region is approximately 0.06 V. At potentials more positive than 0.2 V, a passivation region with a width of 0.2–0.4 V is observed. In this case, the passivation current density is 3.2×10^{-4} A/cm^2. The potential range after 0.4 V is characterized by a rather active anodic process for both Ni–Sn and Ni–Sn–TiO_2 samples. As follows from the polarization curves,

Table 1. Properties of Ni–Sn and Ni–Sn–TiO_2 coatings

	Ni–Sn	Ni–Sn–TiO_2
Microhardness, HV	405	439
Adhesion, MPa/cm^2	0.51	0.65

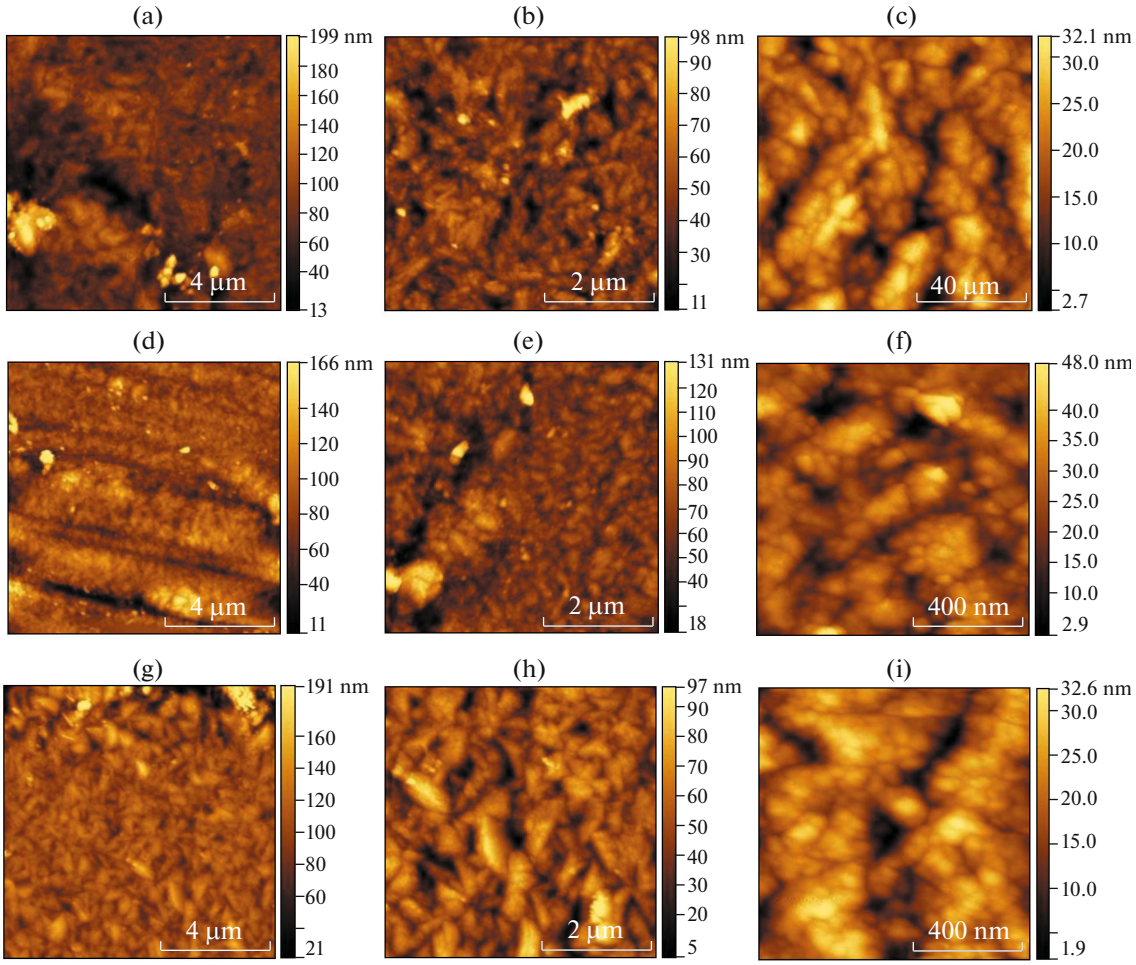

Fig. 2. AFM topography images of Ni–Sn and Ni–Sn–TiO_2 coatings. Concentration of TiO_2 in deposition electrolyte, g/L: (a–c) 0, (d–f) 1, and (g–i) 2.

the introduction of titania into the Ni–Sn alloy leads to depassivation of the coating and promotes an increase in the rate of the anodic process.

The characteristics of corrosion processes in the 3% sodium chloride solution were calculated from the polarization curves and summarized in Table 2. The corrosion current density of samples obtained from the electrolyte with TiO_2 content of 2 g/L decreases to 2.41×10^{-8} as compared to 5.41×10^{-8} A/cm^2 for the coating without titania.

The electrochemical impedance spectroscopy spectra (Fig. 4) also indicated higher corrosion resistance of Ni–Sn–TiO_2 coatings. The Nyquist plots obtained for both types of coatings in the NaCl medium (Fig. 4a) are characterized by a capacitive semicircle at high and medium frequencies, which is characteristic for processes with a limiting stage of charge transfer at the electrode–electrolyte interface [52–57].

In the Bode plots for the phase angle in the midfrequency region, there is a wide peak, which indicates relatively high values of capacitance and resistance of the coating to corrosion. The diagrams for the impedance modulus (Fig. 4b) show that the charge transfer resistance of coatings obtained in the presence of TiO_2

Table 2. Parameters of corrosion processes of Ni–Sn and Ni–Sn–TiO_2 coatings based on analysis of polarization curves

Coating	b_a, V	a_a, V	$\lvert b_c \rvert$, V	a_c, V	i_{cor}, A/cm^2
Sn–Ni	0.0363	0.2072	0.0345	–0.3073	5.41×10^{-8}
Sn–Ni–TiO_2	0.0354	0.221	0.0278	–0.2604	2.41×10^{-8}

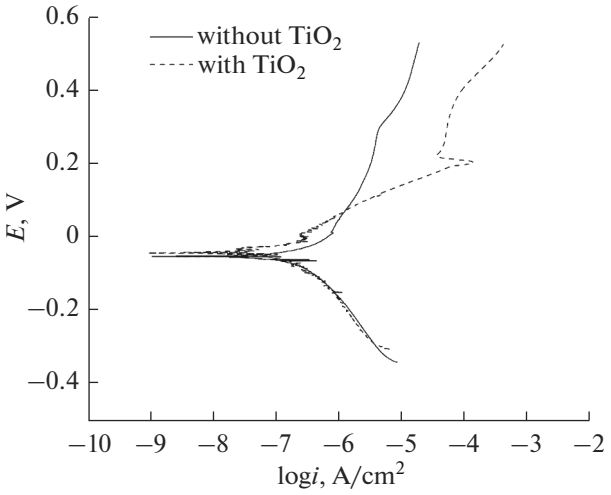

Fig. 3. Potentiodynamic polarization curves of Ni–Sn and Ni–Sn–TiO_2 coatings obtained in a 3% solution of NaCl.

(the low-frequency region) increases from 3.30×10^4 to 8.95×10^4 Ω cm^2.

For a quantitative analysis of the parameters of the spectra obtained, the equivalent circuit shown in Fig. 4 was used. In this circuit, R_s corresponds to the resistance of the corrosive medium, the R_1CPE_1 circuit describes the parameters of the corrosion process in the coating defects, and the R_2CPE_2 circuit describes the charge transfer resistance and the capacity of the electric double layer at the electrode–electrolyte interface. Taking into account the surface roughness, a constant phase element CPE was used in the circuits instead of capacitor element *C*. The results of the fitting of the equivalent circuit parameters are presented in Table 3. For the Ni–Sn–TiO_2 coating, the values of R_1 and R_2 were higher, and for Y_1 and Y_2 lower, than for the Ni–Sn coating, indicating a higher corrosion resistance of the obtained composites. The values of parameter n_1 for both coatings are close to 0.5, which may indicate the occurrence of diffusion processes—probably, in the defective areas of the coatings.

The results of the antibacterial tests of the obtained Ni–Sn and Ni–Sn–TiO_2 coatings toward *S. aureus* and *E. coli* bacteria are shown in Fig. 5. As follows from the experimental data, the presence of titania in the coating significantly reduces the number of bacterial colonies on the surface of the samples. This trend is observed for both *S. aureus* and *E. coli*. The concentration of viable bacteria *S. aureus* on the surface of the samples exposed to UV irradiation with an intensity of 0.01 mV/m^2 for 1 h decreased from 130 to 70 CFU/mL (Table 4). Upon irradiation of coatings obtained from the electrolyte containing 1 g/L of titania, the number of cells decreases from 100 to 20 CFU/mL. This indicates the antibacterial effect of titania, especially when exposed to UV. For the samples obtained in electrolytes with 2 g/L of titania, the antibacterial effect increases by a factor of 1.5 as compared to the control sample.

Such results are most likely due to the photocatalytic antibacterial activity of the Ni–Sn–TiO_2 composite electrochemical coating in the presence of UV radiation [43–45] due to the damage to bacterial cell membranes caused by the absorption of radiation by intracellular chromophores.

The antibacterial activity of the samples to test bacteria during incubation for 4 and 12 h increases with an increase in the titania content in the coating for both *S. aureus* and *E. coli* (Table 5).

Index of antibacterial activity K_2 increases from 1.4 to 1.5 for *E. coli* and from 1.33 to 1.70 for *S. aureus* with an incubation time of 4 h. As the incubation time increases, K_2 also increases, reaching 1.84 for *E. coli* and 2.44 for *S. aureus* at a concentration of titania in electrolyte 2 g/L.

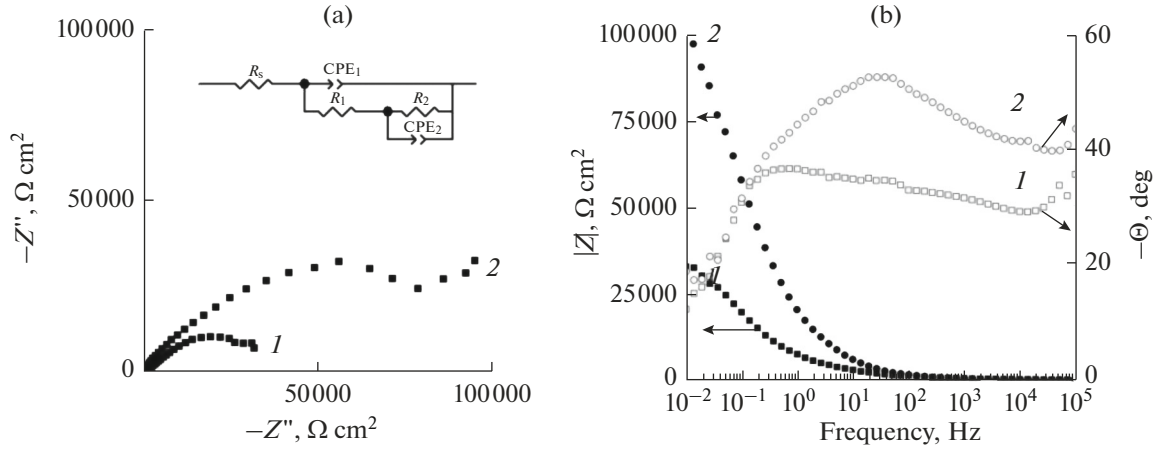

Fig. 4. EIS spectra of (*1*) Ni–Sn and (*2*) Ni–Sn–TiO_2 coatings in 3% NaCl solution in the (a) Nyquist and (b) Bode representation.

Table 3. Parameters of the fitting equivalent circuits elements of Ni–Sn and Ni–Sn–TiO_2 coatings in 3% NaCl solution

Coating	R_s, Ω cm^2	R_1, Ω cm^2	Y_1, Ω^{-1} cm^{-2} s^n	n_1	R_2, Ω cm^2	Y_2, Ω^{-1} cm^{-2} s^n	n_2
Ni–Sn	62.87	3.30×10^4	5.06×10^{-5}	0.42	3.32×10^4	2.0×10^{-5}	1
Ni–Sn–TiO_2	29.78	8.95×10^4	1.63×10^{-5}	0.56	5.36×10^4	9.16×10^{-6}	1

Table 4. Concentration of active *Staphylococcus aureus* of the surface of samples (initial concentration of 5.6×10^5 CFU/mL)

Experimental parameters	Concentration of TiO_2 in electrolyte, g/L	Concentration of bacteria (CFU/mL)	K_1, %
Without UV treatment	0	1.3×10^2	–
	1	1.0×10^2	23.08
	2	9.0×10^1	30.76
After UV treatment (I ~ 0.01 mW/cm^2, 1 h)	0	7.0×10^1	–
	1	2.0×10^1	71.43
	2	3.0×10^1	57.14

CONCLUSIONS

Summarizing, the performed studies have shown that the introduction of nanosized titania into the nickel–tin alloy makes it possible to obtain coatings with increased hardness, adhesion, and corrosion resistance. The microhardness and adhesion of the Ni–Sn–TiO_2 coatings were 439 HV and 0.65 MPa/cm^2, respectively, and the corrosion current density decreased to

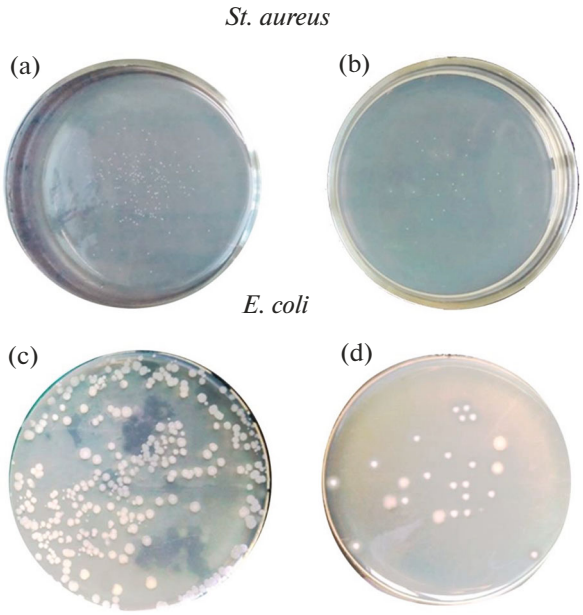

Fig. 5. Optical images of bacteria colonies of (a, b) *St. aureus* and (c, d) *E. coli* after UV treatment with an intensity of 0.01 mW/cm^2 on the surface of (a, c) Ni–Sn and (b, d) Ni–Sn–TiO_2 coatings for 4 h.

Table 5. Antibacterial activity of Ni–Sn and Ni–Sn–TiO_2 coatings against examined bacteria after 4 and 12 h of testing

Concentration of TiO_2 in electrolyte, g/L	*S. aureus*				*E. coli*			
	12 h		4 h		12 h		4 h	
	CFU/mL	K_2	CFU/mL	K_2	CFU/mL	K_2	CFU/mL	K_2
0	2.9×10^7	1.96	2.6×10^4	1.33	2.8×10^7	1.51	2.4×10^4	1.40
1	1.6×10^7	2.23	2.0×10^4	1.44	2.1×10^7	1.64	1.9×10^4	1.50
2	9.8×10^6	2.44	1.0×10^4	1.74	1.3×10^7	1.84	2.1×10^4	1.29
Control sample	2.7×10^9	–	5.6×10^5	–	9.2×10^8	–	6.1×10^5	–

2.41×10^{-8} A/cm^2. The resulting composite coating is characterized by the high biocidal activity against *S. aureus* and *E. coli* bacteria.

FUNDING

This work was financially supported by the Ministry of Education of the Republic of Belarus, project Electrochemical Composite Coatings with Photocatalytic Properties Based on Tin Alloys.

REFERENCES

1. Kaigorodova, T.V., Zimina, E.I., and Ivanov, A.V., *Zdravookhr. Ross. Fed.,* 2009, no. 1, p. 23.
2. *World Health Organization, World Health Statistics 2018: Monitoring Health for the SDGs, Sustainable Development Goals,* Geneva, 2018, p. 64.
3. Beamer, P.I., Plotkin, K.R., Gerba, C.P., et al., *J. Occup. Environ. Hyg.,* 2015, vol. 12, no. 4, p. 266.
4. Julian, T.R.A.O., Canales, R.A.O., Leckie, J.O., et al., *Risk Anal.,* 2009, vol. 29, p. 617.
5. Nicas, M. and Best, D., *J. Occup. Environ. Hyg.,* 2008, vol. 5, p. 347.
6. Lopez, G.U.P.H., Gerba, C.P.H., Tamimi, A.H., et al., *J. Appl. Environ. Microbiol.,* 2013, vol. 79, p. 307.
7. Bartlett, J.G., *Management of Respiratory Tract Infections,* Baltimore, MD: Lippincott Williams and Wilkins, 1997.
8. Zaitsev, A.A., Klochkov, O.I., Mironov, M.B., et al., *Ostrye respiratornye virusnye infektsii: etiologiya, diagnostika, lechenie i profilaktika. Posobie dlya vrachei* (Acute Respiratory Viral Infections: Etiology, Diagnostics, Treatment, and Prevention. Manual for Doctors), Moscow, 2008, p. 37.
9. Bilichenko, T.N. and Chuchalin, A.G., *Ter. Arkh.,* 2018, vol. 90, no. 1, p. 22.
10. Woods, J.B., *Biological Weapons Defense,* Totowa, NJ: Humana Press, 2005, p. 285.
11. Fluit, A.C., Visser, M.R., and Schmitz, F., *Clin. Microbiol. Rev.,* 2001, vol. 14, no. 4, p. 836.
12. Yim, G., Wang, H.H., and Davies, J., *Philos. Trans. R. Soc., B,* 2007, vol. 362, p. 1195.
13. Beloborodov, V.B., *Con. Med.,* 2004, vol. 6, no. 1, p. 18. Beloborodov, V.B., *Consilium Med.,* 2004, vol. 6, no. 1, p. 18.
14. Karkishchenko, N.N., *Biomeditsina,* 2009, no. 1, p. 5.
15. Babushkina, I.V., Borodulin, V.B., Korshunov, G.V., et al., *Sarat. Nauchno-Med. Zh.,* 2010, vol. 6, no. 1, p. 11.
16. Zotova, E.S., *Cand. Sci. (Eng.) Dissertation,* Moscow: *Moscow State Evening Institute* of *Iron and Steel*, 2008.
17. Yin, M., Wu, C.K., Lou, Y., et al., *J. Am. Chem. Soc.,* 2005, vol. 127, no. 26, p. 9506.
18. Reisse, J., Francois, H., Vandercammen, J., et al., *Electrochim. Acta,* 1994, no. 39, p. 37.
19. Eroklintsev, V.N. and Luk'yanova, V.O., *Tendentsii Razvit. Nauki Obraz.,* 2017, no. 28-2, p. 17.
20. Babushkina, I.V., Borodulin, V.B., and Korshunov, G.V., *Klin. Lab. Diagn.,* 2008, no. 9, p. 85.
21. Babushkina, I.V., Borodulin, V.B., Korshunov, G.V., et al., *Sarat. Nauchno-Med. Zh.,* 2010, vol. 6, no. 1, p. 11.
22. Makarova, I.V., Kharitonov, D.S., Dobryden', I.B., et al., *Russ. J. Appl. Chem.,* 2018, vol. 91, p. 1441.
23. Makarova, I., Dobryden', I., Kharitonov, D., et al., *Surf. Coat. Technol.,* 2019, vol. 380, p. 125063.
24. Pyanko, A.V., Makarova, I.V., Kharitonov, D.S., et al., *Inorg. Mater.,* 2019, vol. 55, no. 6, p. 568.
25. Kuznetsov, B.V., Vorobyova, T.N., and Glibin, V.P., *Met. Finish.,* 2013, vol. 111, no. 3, p. 38.
26. Shekhanov, R.F., *Izv. Vyssh. Uchebn. Zaved., Khim. Khim. Tekhnol.,* 2017, vol. 60, no. 10, p. 75.
27. Wagner, V., *Übersichtsstudie Wasserknappheit & Technologie,* Dusseldorf, 2004, p. 194.
28. Park, N.-G., Van de Lagemaat, J., and Frank, A.J., *J. Phys. Chem.,* 2000, vol. 104, no. 38, p. 8989.
29. Smestad, G., Bignozzi, C., and Smestad, R.A., *Sol. Energy Mater. Sol. Cells,* 1994, vol. 32, no. 3, p. 259.
30. Mills, A. and Le Hunte, S., *J. Photochem. Photobiol., A,* 1997, vol. 108, p. 1.
31. Kikuchi, Y., Sunada, K., Iyoda, T., et al., *J. Photochem. Photobiol., A,* 1997, vol. 106, p. 51.
32. Hoffmann, M.R., Martin, S.T., Choi, W., et al., *Chem. Rev.,* 1995, vol. 95, p. 69.
33. Matsunaga, T., Tomoda, R., Nakajima, T., et al., *Appl. Environ. Microbiol.,* 1988, vol. 54, p. 1330.
34. Woods, J.B., *Biological Weapons Defense,* Totowa, NJ: Humana Press, 2005, p. 285.
35. Fluit, A.C., Visser, M.R., and Schmitz, F., *Clin. Microbiol. Rev.,* 2001, vol. 14, no. 4, p. 836.
36. Ollis, D.F. and Al-Ekabi, H., *Open J. Inorg. Chem.,* 1993, p. 511.

37. Xu, M., Huang, N., Xiao, Z., et al., *Supramol. Sci.,* 1998, no. 5, p. 449.
38. Freitas, R.A., Jr., *Int. J. Surg.,* 2005, no. 3, p. 243.
39. Murashkevich, A.N., Alisienok, O.A., Zharskiy, I.M., et al., *J. Sol-Gel Sci. Technol.,* 2019, vol. 92, p. 254.
40. Kutuzau, M., Shumskaya, A., and Kaniukov, E., *Nucl. Instrum. Methods Phys. Res., Sect. B,* 2019, vol. 460, p. 212.
41. Murashkevich, A.N., Chechura, K.M., Novitskaya, M.S., et al., *Inorg. Mater.,* 2018, vol. 54, p. 1223.
42. Kuz'micheva, G.M., Savinkina, E.V., Obolenskaya, L.N., et al., *Crystallogr. Rep.,* 2010, vol. 55, no. 5, p. 866.
43. Ismagilov, Z.R., Tsikoza, L.T., Shikina, N.V., et al., *Russ. Chem. Rev.,* 2009, vol. 78, p. 873.
44. Gerasimenko, Yu.V., Logacheva, V.A., and Khoviv, A.M., *Kondens. Sredy Mezhfaznye Granitsy,* 2010, vol. 12, no. 2, p. 113.
45. Kim, B., Kim, D., Cho, D., et al., *Chemosphere,* 2003, vol. 52, p. 277.
46. Modesa, T., Scheffela, B., Metznera, Chr., et al., *Surf. Coat. Technol.,* 2005, vol. 200, p. 306.
47. Kleiman, A., Mrquez, A., and Lamas, D.G., *Surf. Coat. Technol.,* 2007, vol. 201, p. 86.
48. Nishimoto, S., Ohtani, B., Kaijiwara, H., et al., *J. Chem. Soc., Faraday Trans. 1,* 1985, vol. 81, p. 61.
49. Kovalenko, I.V., Chernenko, L.V., Khainakov, S.A., et al., *Ukr. Khim. Zh.,* 2008, vol. 74, nos. 3–4, p. 52.
50. Kovalenko, I.V., *Cand. Sci. (Chem.) Dissertation,* Kyiv, 2009.
51. Kuznetsov, B.V., Vorobyova, T.N., and Glibin, V.P., *Met. Finish.,* 2013, vol. 111, no. 3, p. 38.
52. Antikhovich, I.V., Kharitonov, D.S., Chernik, A.A., et al., *Russ. J. Appl. Chem.,* 2017, vol. 90, no. 4, p. 566.
53. Winiarski, J., Niciejewska, A., Ryl, J., et al., *Materials,* 2020, vol. 13, p. 924.
54. Wysocka, I., Kowalska, E., Ryl, J., et al., *Nanomaterials,* 2019, vol. 9, p. 1129.
55. Miszczyk, A. and Darowicki, K., *Anti-Corros. Methods Mater.,* 2011, vol. 58, no. 1, pp. 13–21.
56. Rudoy, V.M., Ostanin, N.I., Ostanina, T.N., et al., *Russ. J. Non-Ferrous Met.,* 2019, vol. 60, pp. 632–638.
57. Nikitin, V.S., Rudoi, V.M., Ostanina, T.N., et al., *J. Anal. Chem.,* 2017, vol. 72, pp. 390–395.

Translated by D. Kharitonov